

A constitutive approach to fracture simulation based on augmented virtual internal bond method

Zhennan Zhang^{*}, Shaofeng Yao

School of Naval Architecture, Ocean and Civil Engineering, Shanghai Jiao Tong University, Shanghai, 200240, China

* Corresponding author: zhennanzhang@sjtu.edu.cn

Abstract The K-dominant zone, which is a small area surrounding the fracture tip, has been the interesting focus of the fracture mechanics. In the traditional linear elastic fracture mechanics(LEFM), a stress intensity factor is used to characterize the stress field of the K-dominant zone and a separate fracture criterion is used to predict the fracture behaviors. However, when using LEFM to simulate fracture propagation, the computation of stress intensity factor is a tough problem. The LEFM is actually a phenomenological methodology. The fracture behaviors are determined by material microstructure. The augmented virtual internal bond(AVIB) is a constitutive model based on microstructure. Its constitutive relation is derived from the micro bond potential, which contains the micro fracture mechanism. Hence, the so-called fracture criterion is implicitly built in the constitutive relation. In this paper, the AVIB constitutive model is used in the K-dominant zone while the usual linear elastic constitutive model is used in the rest zone to simulate fracture propagation. By this method, the computation of stress intensity factor is avoided. When and how fracture propagation is completely governed by the AVIB constitutive relation. It provides an efficient approach to fracture simulation.

Keywords Fracture simulation, Augmented virtual internal bond, Constitutive model, Microstructure

1. Introduction

In the methodology of linear elastic fracture mechanics(LEFM), the singular mechanical field of crack tip is characterized by the so-called stress intensity factors (SIFs). Whether fracture propagates is governed by SIF and material fracture toughness. So, many fracture criteria in terms of SIFs have been proposed. When using FEM to simulate fracture behaviors, the SIF is a key factor that has to be calculated. However, the computation of SIF is a tough problem in computational mechanics, which requires very fine mesh scheme at vicinity of crack tip or special treatment on mesh scheme. The cohesive surface methodology pioneered by Barenblatt[1] and Dugdale[2] take a different philosophy to deal with the fracture tip problem. It is assumed that there is a cohesive zone ahead of crack tip, which is governed by a cohesive law. The cohesive law is characterized by the cohesive strength and the fracture energy. When using this method, the stress intensity problem, therefore the SIF problem, is avoided. However, in FEM simulation, a cohesive zone is usually inserted into the bulk material, which brings inconvenience to numerical procedure. In the present paper, the cohesive properties of microstructure at vicinity of crack tip are directly built in the constitutive relation through augmented virtual internal bond(AVIB)[3] model. Hence, in the present simulation strategy, only at the K-dominant zone is the AVIB constitutive model used while at the rest zone, the linear elastic constitutive model is used. The present method is suggested highly efficient, avoiding the SIF computation and fracture criteria problem.

2. Constitutive relation of material at vicinity of crack tip

Before the deformation of material reaches its linear elastic limit, the linear elastic continuum constitutive relation can well describe the behaviors of material. However, once the deformation exceeds this limit, the conventional continuum constitutive model couldn't well describe it. In such situation, the augmented virtual internal bond(AVIB)[3] is an effective approach to address this

problem. Hence, the idea of the present method can be depicted by Fig.1. At the K-dominant zone which experience large deformation, the AVIB constitutive model is used while at the rest zone where the deformation is small, the linear elastic constitutive model is adopted.

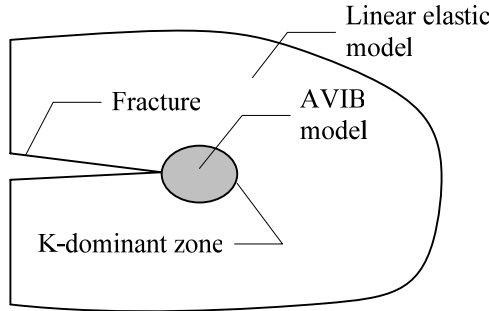


Fig.1 Depiction of the constitutive approach to fracture simulation.

In VIB theory[4], the solid is considered to consist of randomized discrete material particles on micro scale and the constitutive relation is directly derived from the interactions between material particles. The AVIB generalizes the original VIB model in that the shear deformation effect between material particles is considered via Xu-Needleman potential. Therefore, the AVIB can represent material with different Poisson ratios. The micro structure of AVIB is shown in Fig.1.

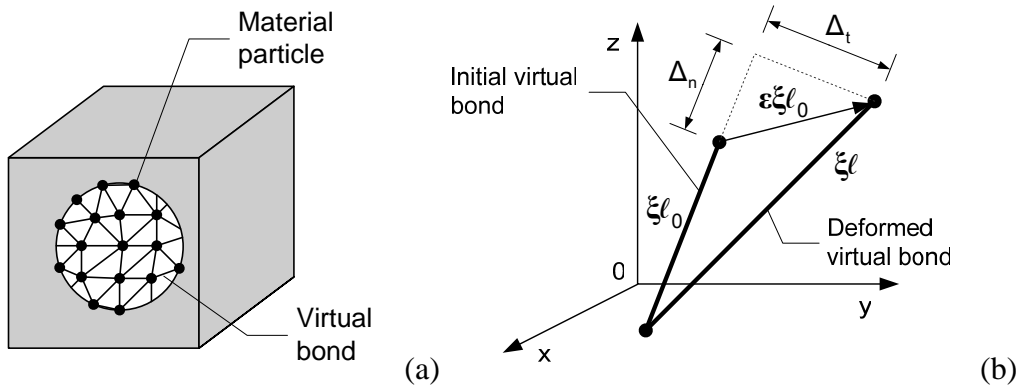


Fig.2 Micro structure of AVIB and micro bond deformation (ϵ denotes the strain tensor; ξ the bond orientation vector; l_0 the original bond length)

The micro bond can be described by the following simplified Xu-Needleman potential[5]

$$U(\Delta) = \phi_n - \phi_n \exp\left(-\frac{\Delta_n}{\delta_n}\right) \left(1 + \frac{\Delta_n}{\delta_n}\right) \left[1 - q + q \exp\left(-\frac{\Delta_t^2}{\delta_t^2}\right)\right] \quad (1)$$

where Δ_n, Δ_t are respectively the normal and shear bond deformation. In AVIB, they are calculated as

$$\begin{aligned} \Delta_n &= \xi^T \epsilon \xi l_0 \\ \Delta_t^2 &= \left[\xi^T \epsilon^T \epsilon \xi - (\xi^T \epsilon \xi)^2 \right] l_0^2 \end{aligned} \quad (2)$$

Based on Eq.(2), define the second-order tensor \mathbf{N} , \mathbf{P} and the forth-order tensor \mathbf{Q} respectively as

$$\begin{aligned} N_{ij} &= \frac{1}{l_0} \cdot \frac{\partial \Delta_n}{\partial \varepsilon_{ij}} = \xi_i \xi_j \\ P_{ij} &= \frac{1}{l_0^2} \cdot \Delta_t \cdot \frac{\partial \Delta_t}{\partial \varepsilon_{ij}} = \varepsilon_{ip} \xi_p \xi_j - (\xi^T \mathbf{e} \xi) \xi_i \xi_j \\ Q_{ij} &= \frac{1}{l_0^2} \cdot \left(\frac{\partial \Delta_t}{\partial \varepsilon_{kl}} \cdot \frac{\partial \Delta_t}{\partial \varepsilon_{ij}} + \Delta_t \frac{\partial^2 \Delta_t}{\partial \varepsilon_{ij} \partial \varepsilon_{kl}} \right) = \delta_{ik} \xi_j \xi_l - \xi_i \xi_j \xi_k \xi_l \end{aligned} \quad (3)$$

where δ_{ij} being the Kronecker delta.

According to this micro structure, the strain tensor of material[3] can be derived as

$$\sigma_{ij} = \frac{\partial \Phi}{\partial \varepsilon_{ij}} = \frac{1}{V} \left\langle \frac{\partial U}{\partial \Delta_n} \cdot \frac{\partial \Delta_n}{\partial \varepsilon_{ij}} + \frac{\partial U}{\partial \Delta_t} \cdot \frac{\partial \Delta_t}{\partial \varepsilon_{ij}} \right\rangle \quad (4)$$

and the tangent modulus of material as

$$\begin{aligned} C_{ijkl} &= \frac{\partial^2 \Phi}{\partial \varepsilon_{ij} \partial \varepsilon_{kl}} = \frac{1}{V} \left\langle \frac{\partial^2 U}{\partial \Delta_n^2} \cdot \frac{\partial \Delta_n}{\partial \varepsilon_{kl}} \cdot \frac{\partial \Delta_n}{\partial \varepsilon_{ij}} + \frac{\partial U}{\partial \Delta_n} \cdot \frac{\partial^2 \Delta_n}{\partial \varepsilon_{ij} \partial \varepsilon_{kl}} \right. \\ &\quad \left. + \frac{\partial^2 U}{\partial \Delta_t^2} \cdot \frac{\partial \Delta_t}{\partial \varepsilon_{kl}} \cdot \frac{\partial \Delta_t}{\partial \varepsilon_{ij}} + \frac{\partial U}{\partial \Delta_t} \cdot \frac{\partial^2 \Delta_t}{\partial \varepsilon_{ij} \partial \varepsilon_{kl}} \right. \\ &\quad \left. + \frac{\partial^2 U}{\partial \Delta_n \partial \Delta_t} \cdot \frac{\partial \Delta_t}{\partial \varepsilon_{kl}} \cdot \frac{\partial \Delta_n}{\partial \varepsilon_{ij}} + \frac{\partial^2 U}{\partial \Delta_t \partial \Delta_n} \cdot \frac{\partial \Delta_n}{\partial \varepsilon_{kl}} \cdot \frac{\partial \Delta_t}{\partial \varepsilon_{ij}} \right\rangle \end{aligned} \quad (5)$$

in which Φ denotes the strain energy density of a micro element; ε the strain tensor; V the volume of the micro element and $\langle \mathbf{L} \rangle = \int_0^{2\pi} \int_0^\pi (\mathbf{L}) D(\theta, \phi) \sin \theta d\theta d\phi$ in spherical coordinates for 3D case and $\langle \mathbf{L} \rangle = \int_0^{2\pi} (\mathbf{L}) D(\theta) d\theta$ for 2D case.

Substituting Eqs.(1,2,3) into Eqs.(4,5), the stress tensor and tangent modulus tensor can be rewritten as

$$\sigma_{ij} = \frac{1}{V} \left\langle f_n \cdot N_{ij} + f_t \cdot P_{ij} \right\rangle \quad (6)$$

and

$$C_{ijkl} = \frac{1}{V} \left\langle f_A \cdot N_{ij} N_{kl} + f_B \cdot Q_{ijkl} - f_C \cdot P_{ij} P_{kl} - f_D \cdot (P_{ij} N_{kl} + N_{ij} P_{kl}) \right\rangle \quad (7)$$

in which the coefficients are respectively

$$\begin{aligned}
 f_n &= A_0 \cdot c_1 c_3 \cdot \frac{\Delta_n}{l_0}, & f_t &= B_0 \cdot c_1 c_2 c_4 \\
 f_A &= A_0 \cdot c_1 c_3 c_5, & f_B &= B_0 \cdot c_1 c_2 c_4 \\
 f_C &= B_0 \cdot c_1 c_2 c_4 \cdot \frac{2l_0^2}{\delta_t^2}, & f_D &= B_0 \cdot c_1 c_2 \cdot \frac{l_0 \Delta_n}{\delta_n^2}
 \end{aligned} \tag{8}$$

The coefficient in Eq.(8) are respectively

$$\begin{aligned}
 A_0 &= \frac{\phi_n l_0^2}{\delta_n^2}, & B_0 &= \frac{2q\phi_n l_0^2}{\delta_t^2}, & c_1 &= \exp\left(-\frac{\Delta_n}{\delta_n}\right), & c_2 &= \exp\left(-\frac{\Delta_t^2}{\delta_t^2}\right) \\
 c_3 &= 1 - q + q \cdot c_2, & c_4 &= 1 + \frac{\Delta_n}{\delta_n}, & c_5 &= 1 - \frac{\Delta_n}{\delta_n}
 \end{aligned} \tag{9}$$

In [3], Zhang and Gao proposed a remedy method for element size sensitivity, which essentially embedded the fracture energy into the constitutive relation. By adjusting the material parameters at fracture tip, AVIB can keep the strain energy release rate constant. According to the idea of AVIB, the adjusted parameters at crack tip is

$$\hat{A}_0 = A_0 / \lambda, \quad \hat{B}_0 = B_0 / \lambda, \quad \hat{\delta}_n = \lambda \delta_n, \quad \hat{\delta}_t = \lambda \delta_t \tag{10}$$

where λ is the adjustment coefficient. The adjustment coefficient takes the following values for different cases.

$$\lambda = \begin{cases} \lambda = \frac{2J(1-2\nu)}{3\pi h E \varepsilon_t^2} & \text{for 3D} \\ \lambda = \frac{J(1-\nu)}{2h E \varepsilon_t^2} & \text{for 2D-stress} \\ \lambda = \frac{J(1+\nu)(1-2\nu)}{2h E \varepsilon_t^2} & \text{for 2D-strain} \end{cases} \tag{11}$$

in which J is the intrinsic J-integral of material; h is the element size, as

$$h = c\sqrt{S} \tag{12}$$

where S is the area of an element and c is a geometrical factor. In the numerical examples discussed in the next section, take $c = 4\sqrt{2}$.

3 . Criterion of crack tip element

When using the present method, it is necessary to identify the element of crack tip. Usually, the

crack tip element deformation is very large. Hence, to detect the crack tip element, the following criterion is adopted in the present paper.

$$\varepsilon_1 > \varepsilon_t \quad (13)$$

In which ε_1 is the first principle eigenstrain value of strain tensor.

4 . simulation example

To show the validation of the present method, a three-point-bending(TPB) test reported in[6] is presented simulated. The material parameters provided by [6] are: the Young's modulus $E = 30.5$ GPa, Poisson ratio $\nu = 0.2$; tensile strength $f_t = 3.8$ MPa and fracture energy $G_f = 62.5$ N/m. With these parameters, the calibrated parameters are $\varepsilon_t = 0.2486 \times 10^{-3}$ and $\varepsilon_c = 2.486 \times 10^{-3}$. The specimen, boundary conditions and mesh configuration are shown in Fig.3. The displacement controlling loading scheme is adopted. Each step is 0.002486 mm.

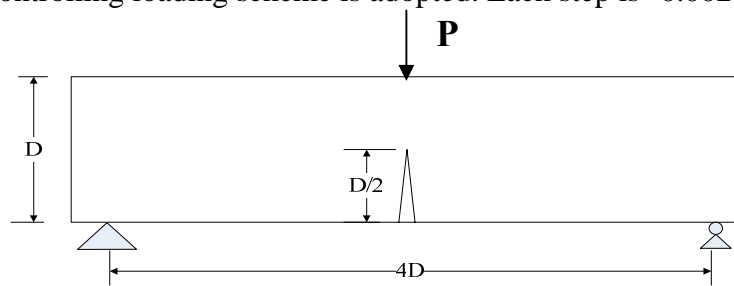


Fig.3 The specimen and boundary conditions of TPB test. $D = 0.075$ m and the sample thickness is 0.05m.

The simulation results are shown in Fig.4 and Fig.5. From Fig.4, it is seen that crack propagates gradually with loading increasing. The propagation pattern agrees with the observation in the experiment[6]. Fig.5 shows the comparison between the experimental and the simulated results. From Fig.6 it is seen that the present method can well predict the fracture propagation, free of the element size sensitivity problem.

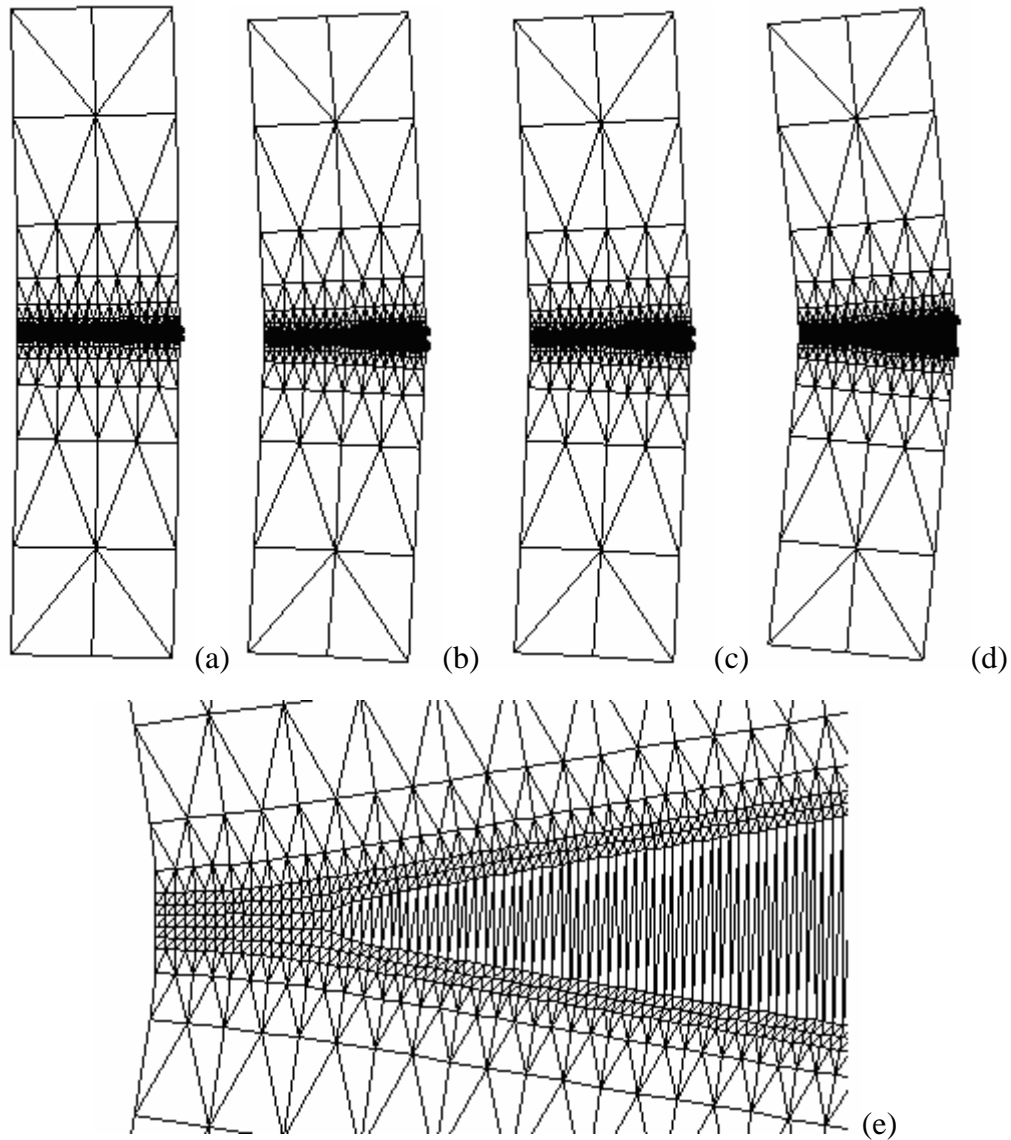


Fig.4 Crack propagation process (a) Step = 6; (b) Step = 16; (c) Step = 30; (d) Step = 50; (e) Crack tip zone zoomed in at Step =50. (Node displacement is magnified 200 times.)

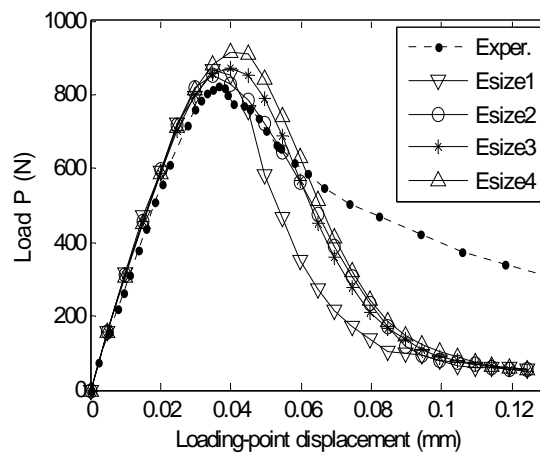


Fig.5 Comparison between the simulated load-displacement curves and the experimental results. ('Exper.' denotes the experimental results. The beam is discretized into N segments along the width in the middle cross section of beam. Esize1, Esize2, Esize3 and Esize4 correspond to the segment number 32, 64, 128, and 256, respectively.)

5 .Conclusion remarks

At the K-dominant zone, a micro-macro cohesive constitutive model is used while at the rest zone, the linear elastic constitutive model is used. By this method, the fracture propagation can well be predicted. The simulation example suggests that the present method is validated. By the present method, the fracture criterion is directly built in the constitutive model. It avoids the choice of separate fracture criterion problem and the computation of stress intensity factor, which brings great convenience to fracture simulation.

Acknowledgement:

The present work is supported by National Natural Science Foundation of China (No. 11172172), which is gratefully acknowledged.

References

- [1] Barenblatt, G.I., The formulation of equilibrium cracks during brittle fracture: General ideas and hypotheses, axially symmetric cracks. *Appl. Math. Mech.(PMM)*, 23(1959) 622-636.
- [2] Dugdale, D.S., Yielding of steel sheets containing slits. *Journal of mechanics and physics of solids*, 8(2)(1960) 100-104.
- [3] Zhang, Z.N. and H.J. Gao, Simulating fracture propagation in rock and concrete by an augmented virtual internal bond method. *International Journal for Numerical and Analytical Methods in Geomechanics*, 36 (4)(2012) 459-482.
- [4] Gao, H.J. and P. Klein, Numerical simulation of crack growth in an isotropic solid with randomized internal cohesive bond. *Journal of the Mechanics and Physics of Solids*, 46(2)(1998) 187-218.
- [5] Xu, X.P. and A. Needleman, Numerical simulations of fast crack growth in brittle solids. *Journal of Mechanics and Physics of Solids*, 42(1994) 1397-1434.
- [6] Yu, R.C., G. Ruiz, and E.W.V. Chaves, A comparative study between discrete and continuum models to simulate concrete fracture. *Engineering Fracture Mechanics*, 75(2008) 117-127.